Benajes Calvo, JV.; Molina, S.; García Martínez, A.; Monsalve Serrano, J. (2015). Effects of direct injection timing and blending ratio on RCCI combustion with different low reactivity fuels. Energy Conversion and Management. 99:193-209. doi:10.1016/j.enconman.2015.04.046.

Effects of Direct injection timing and Blending Ratio on RCCI combustion with different Low Reactivity Fuels

Energy Conversion and Management, Volume 99, 2015, Pages 193–209.
http://dx.doi.org/10.1016/j.enconman.2015.04.046

Jesús Benajes, Santiago Molina, Antonio García*, Javier Monsalve-Serrano

CMT - Motores Térmicos, Universitat Politècnica de València, Camino de Vera s/n,

46022 Valencia, Spain

(*) CORRESPONDING AUTHOR:

Dr. Antonio García: angarma8@mot.upv.es

Telephone: +34 963879659

Fax: +34 963877659

Abstract

This work investigates the effects of the direct injection timing and blending ratio on RCCI performance and engine-out emissions at different engine loads using four low reactivity fuels: E10-95, E10-98, E20-95 and E85 (port fuel injected) and keeping constant the same high reactivity fuel: diesel B7 (direct injected). The experiments were conducted using a heavy-duty single-cylinder research diesel engine adapted for dual-fuel operation. All the tests were carried out at 1200 rpm. To assess the blending ratio effect, the total energy delivered to the cylinder coming from the low reactivity fuel was kept constant for the different fuel blends investigated by adjusting the low reactivity fuel mass as required in each case. In addition, a detailed analysis of the air/fuel mixing process has been developed by means of a 1-D in-house developed spray model.

Results suggest that notable higher diesel amount is required to achieve a stable combustion using E85. This fact leads to higher NOx levels and unacceptable ringing intensity. By contrast, EURO VI NOx and soot levels are fulfilled with E20-95, E10-98 and E10-95. Finally, the higher reactivity of E10-95 results in a significant reduction in CO and HC emissions, mainly at low load.

Keywords

Reactivity Controlled Compression Ignition; Engine-out emissions; mixing process; Efficiency; EURO VI

1. Introduction

The stringent regulations introduced around the world to limit the pollutant emissions of internal combustion engines (ICE) present a major challenge for the engine research community. In spite of its efficiency, conventional mixing-controlled diesel combustion

in CI diesel engines requires complex and costly exhaust aftertreatment systems to reach the NOx and soot limitation values proposed in the current regulations, such as EURO VI. Specifically, the rich local equivalences ratios and the high temperatures achieved during the conventional diesel combustion (CDC) as well as the oxygen availability in the outside of the spray plume results in an unacceptable emissions [1]. Additionally to the complexity of the aftertreatment systems, the use of DPF (to reduce soot emissions) and LNT or SCR (to minimize NOx emissions) requires a periodically regeneration (operating rich) or the introduction of a reducing agent, which penalizes the fuel consumption. Thus, in order to reduce aftertreatment costs and fuel consumption it is necessary to avoid the generation of these pollutants in the focus of the emission, i.e. during the combustion development.

Many new compression ignition combustion strategies have been proposed to simultaneously improve the engine efficiency while reducing the NOx and soot emission levels under the regulation limits [2]. The more promising combustion strategies are the well-known low temperature combustion (LTC) strategies. A widely investigated combustion strategy is homogeneous charge compression ignition (HCCI), which produces virtually no soot or NOx emissions while maintaining high efficiency [3]. However, this combustion process presents some challenges with regard to combustion control and engine stress. Thus, due to the rapid heat release, steep pressure gradients occur so that the process has been limited to use within the partial load range [4]. On this regard, Bessonette et al. [5] suggested that different in-cylinder reactivity is required for the proper HCCI operation under different operating conditions. Specifically, high cetane fuels are required at low load and a low cetane fuel are needed at medium-high load.

With the aim of improving the HCCI shortcomings in terms of controllability and knocking, the use of fuels with lower reactivity than diesel fuel (gasoline-like fuels) under Partially Premixed Combustion (PPC) strategies has been widely investigated [6][7]. The investigations confirmed gasoline PPC as a promising method to control the heat release rate providing a reduction in NOx and soot emissions [8]. Thus, by injecting the fuel later in the engine cycle than in HCCI strategy, the air-fuel mixing degree is reduced and therefore higher control on the ignition delay as well as the combustion duration is achieved. Additionally, the use of gasoline fuel provides more flexibility to achieve the required extra mixing time at medium-high loads [9]. However, the concept has demonstrated difficulties at low load conditions [10][11] using gasoline with octane number (ON) greater than 90. With the aim of improving the PPC cycle-to-cycle control at low loads using high ON gasolines, PPC spark assisted concept has been studied [12][13]. It has been demonstrated that the spark assistance provides temporal and spatial control over the combustion process [14], however the high local reactivity required between the spark plug electrodes at the start of spark timing and the flame propagation process result in an unacceptable NOx and soot emissions [15]. In this sense, the double injection strategy applied to the PPC spark assisted concept has been confirmed as a suitable strategy to improve the unburned HC and CO emissions, but still do not solve the unacceptable NOx and soot emission levels [16][17].

Experimental and numerical studies demonstrated that Reactivity Controlled Compression Ignition (RCCI) combustion is a more promising LTC technique than HCCI and PPC [18]. RCCI concept is a partially premixed combustion strategy based on dual-fuel operation. To delivery both fuels separate injection systems for the low reactivity

and high reactivity fuel are used, being port fuel injected (PFI) and direct injected (DI) respectively. Thus, a flexible operation over a wide operating range is possible by modifying both, the low reactivity fuel percentage in the blend and the direct injection timing [19]. The variation of these engine settings provides the required in-cylinder equivalence ratio and reactivity (i.e. octane number) stratification [20][21]. Several studies confirm that in order to achieve high efficiency while reducing NOx and soot emissions, the higher portion of the energy should come from the low reactivity fuel [22][23]. Taking into account this statement, it is clear that the low reactivity fuel characteristics and its amount in the blend have a significant contribution to the in-cylinder reactivity, and therefore, to the combustion development and its emissions. In this sense, recent works investigated the use of E85 fuel as alternative of gasoline on RCCI concept [24][25][26][27]. In terms of emissions, the use of E85 resulted in increased HC and CO levels with decreased NOx. On the other hand, the operating range was found limited by an excessive pressure rise rates at a certain E85 percentages and by misfire conditions when high portions of E85 were used. Thus, the main objective of the present work is to evaluate the potential of various low reactivity fuels with different ethanol content and gasoline octane number on RCCI performance and engine-out emissions at low, medium and high engine loads. For this purpose, the direct injection timing and blending ratio has been sweep using four different low reactivity fuels and keeping constant the same high reactivity fuel. Moreover, to understand the differences in the combustion behavior among the different fuel blends, a detailed analysis of the air/fuel mixing process has been developed by means of a 1-D spray model. Finally, to suggest the proper low reactivity fuel for the RCCI

conditions proposed in this research, a direct comparison of the results obtained with each fuel blend is done taking into account certain constraints.

2. Experimental Facilities and Processing Tools

2.1. Experimental setup

2.1.1. Test cell, engine description and instrumentation

A single cylinder, HD diesel engine representative of commercial truck engine, has been used for all experiments in this study. Detailed specifications of the engine are given in Table 1.

Table 1. Single cylinder engine specifications.

Bore x Stroke [mm]	123 x 152
Connecting rod length [mm]	225
Displacement [L]	1.806
Geometric compression ratio [-]	14.4:1
Bowl Type	Open crater
Number of Valves	4
IVO	375 CAD ATDC
IVC	535 CAD ATDC
EVO	147 CAD ATDC
EVC	347 CAD ATDC

The engine was installed in a fully instrumented test cell, with all the auxiliary facilities required for its operation and control, as it is illustrated in Figure 1.

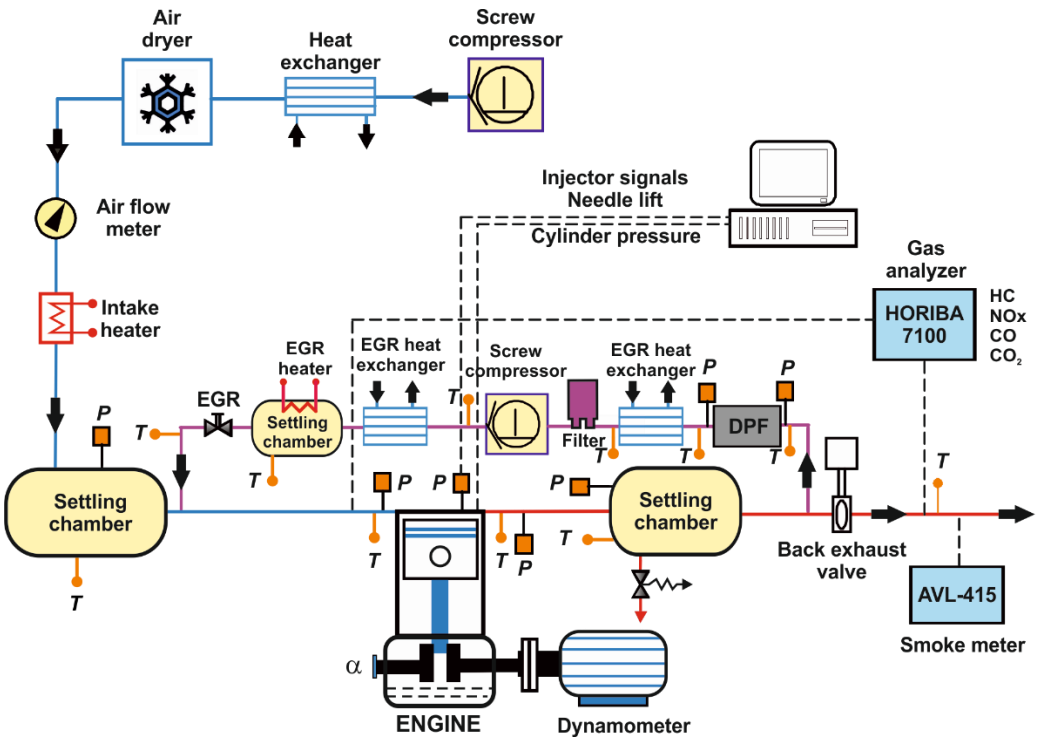

Figure 1. Complete test cell setup.

Moreover, to achieve stable intake air conditions, a screw compressor supplied the required boost pressure before passing through an air dryer. The air pressure was adjusted within the intake settling chamber, while the intake temperature was controlled in the intake manifold after mixing with the EGR flow. The exhaust backpressure produced by the turbine in the real engine was replicated by means of a valve placed in the exhaust system, controlling the pressure in the exhaust settling chamber. Low pressure EGR was produced taking exhaust gases from the exhaust settling chamber. The determination of the EGR rate was carried out using the experimental measurement of intake and exhaust CO_2 concentration. The concentrations of NOx, CO, unburned HC, intake and exhaust CO_2, and O_2 were analyzed with a five gas Horiba MEXA-7100 DEGR analyzer bench by averaging 40 seconds after attaining steady state operation. CO and unburned HC measurements were used to determine the combustion efficiency as:

$$\text{Comb. Eff} = \left(1 - \frac{\text{HC}}{\text{mf}} - \frac{\text{CO}}{4 \cdot \text{mf}}\right) \cdot 100$$

(1)

Smoke emission were measured with an AVL 415S Smoke Meter and averaged between three samples of a 1 liter volume each with paper-saving mode off, providing results directly in FSN (Filter Smoke Number) units. PM measurements of FSN were transformed into specific emissions (g/kWh) by means of the factory AVL calibration. Finally, the in-cylinder pressure signal was measured with a Kistler 6125C pressure transducer coupled with a Kistler 5011B10 charge amplifier. A shaft encoder with 1800 pulses per revolution, which provides a resolution of 0.2 CAD, was used.

2.1.2. Fuels and fuels delivery

The experimental tests were carried out using commercially available diesel and four different low reactivity fuels. The LRFs were selected in order to assess the influence of the ethanol content with the same gasoline (E10-95 and E20-95), the influence of the gasoline ON with a fixed ethanol content (E10-95 and E10-98) and finally, the influence of a fuel mainly composed of ethanol (E85) on RCCI capabilities. Thus, their main properties related with auto-ignition are listed in Table 2. All the properties were obtained following ASTM standards.

Table 2. Physical and chemical properties of the fuels used along the study.

	Diesel B7	E10-95	E20-95	E10-98	E85
Density [kg/m^3] (T= 15 °C)	837.9	739	745	755	781
Viscosity [mm^2/s] (T= 40 °C)	2.67	-	-	-	-
RON [-]	-	98.8	99.1	103	108
MON [-]	-	85.2	85.6	90	89
Ethanol content by volume [%]	-	9.7	19.7	9.7	84.7
Cetane number [-]	54	-	-	-	-
Lower heating value [kJ/kg]	42.61	41.32	40.05	41.29	31.56

To enable RCCI operation the engine was equipped with a double injection system, as it is shown in the scheme of Figure 2. This injection hardware enables to vary the in-cylinder fuel blending ratio and fuel mixture properties according to the engine operating conditions.

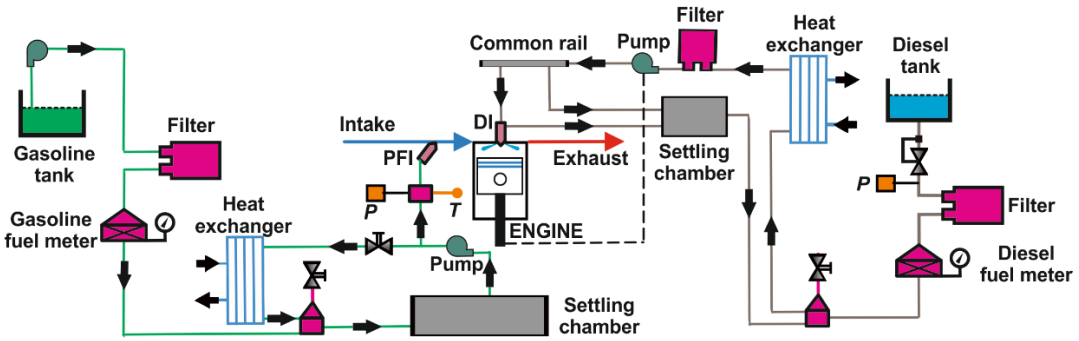

Figure 2. Fuel injection systems scheme.

To inject the diesel fuel, the engine was equipped with a common-rail flexible injection hardware which is able to perform up to five injections per cycle; the main characteristic of this hardware is its capability to amplify common-rail fuel pressure for one of the injections by means of a hydraulic piston directly installed inside the injector. The main characteristics of the injector and nozzle used are depicted in Table 3.

Table 3. Main characteristics of the high reactivity fuel injector.

Actuation Type	Solenoid
Steady flow rate @ 100 bar [cm^3/s]	28.56
Number of Holes	7
Hole diameter [µm]	194
Included Spray Angle [°]	142

Concerning the low reactivity fuel injection, an additional fuel circuit was in-house developed with a reservoir, fuel filter, fuel meter, electrically driven pump, heat exchanger and a commercially available port fuel injector (PFI). The mentioned injector was located at the intake manifold and was specified to be able to place all the low

reactivity fuel into the cylinder during the intake stroke. Consequently, the injection timing was fixed 10 CAD after the IVO to allow the fuel to flow along 160 mm length (distance from PFI location to intake valves seats). Accordingly, this set up would avoid fuel pooling over the intake valve and the undesirable variability introduced by this phenomenon. The main characteristics of the port fuel injector are depicted in Table 4.

Table 4. Main characteristics of the low reactivity fuel injector.

Injector Style	Saturated
Steady flow rate @ 3 bar [cm^3/min]	980
Included Spray Angle [°]	30
Injection Pressure [bar]	5.5
Injection Strategy	Single
Start of Injection Timing	385 CAD ATDC

2.2. Theoretical tools

2.2.1. Analysis of in-cylinder pressure signal

The combustion analysis was performed with an in-house one-zone model named CALMEC, which is fully described in [28]. This combustion diagnosis tool uses the in-cylinder pressure signal and some mean variables (engine speed, coolant, oil, inlet and exhaust temperatures, air, EGR and fuel mass flow…) as its main inputs.

The pressure traces from 150 consecutive engine cycles were recorded in order to compensate the cycle-to-cycle variation during engine operation. Thus, the individual pressure data of each engine cycle was smoothed using a Fourier series low-pass filter. Once filtered, the collected cycles were ensemble averaged to yield a representative cylinder pressure trace, which was used to perform the analysis. Then, the first law of thermodynamics was applied between IVC and EVO, considering the combustion chamber as an open system because of the blow-by and fuel injection. The ideal gas equation of state was used to calculate the mean gas temperature in the chamber. In

addition, the in-cylinder pressure signal allowed obtaining the gas thermodynamic conditions in the chamber to feed the convective and radiative heat transfer models [29], as well as the filling and emptying model that provided the fluid-dynamic conditions in the ports, and thus the heat transfer flows in these elements. The convective and radiative models are linked to a lumped conductance model to calculate the wall temperatures.

The main result of the model used in this work was the Rate of Heat Release (RoHR). Moreover, several parameters were calculated from the RoHR profile. In particular, Start of combustion (SoC) was defined as the crank angle position in which the cumulated heat release reached a value of 2% and combustion phasing was defined as the crank angle position of 50% fuel mass fraction burned (CA50). Additionally, ringing intensity was calculated by means of the correlation of Eng [30]:

$$\mathrm{RI} = \frac{1}{2\gamma}\frac{[0.05 \cdot (\mathrm{dP/dt})_{\max}]^2}{\mathrm{P_{max}}}\sqrt{\gamma \mathrm{R T_{max}}}$$

(2)

Where γ is the ratio of specific heats, $(dP/dt)_{max}$ is the peak PRR, P_{max} is the maximum of in-cylinder pressure, R is the ideal gas constant, and T_{max} is the maximum of in-cylinder temperature.

2.2.2. Analysis of mixing process

The data derived from the SCE were used as input for an in-house 1-D spray model, DICOM [31][32]. The main objective when applying the code is to clarify the mixing process in response to variations of the in-cylinder fuel blending and direct injection timing. The main specific inputs for the model are the instantaneous in-cylinder pressure, the spray cone angle, as well as the density and the instantaneous injection

rate, which are obtained from CALMEC. In order to take into account the fresh air, EGR rate and the low reactivity fuel entrainment, two additional inputs are also needed for the 1-D model; the oxygen mass fraction at IVC and the stoichiometric equivalence ratio of the in-cylinder fuel blend [33]:

$$\phi_{est} = \frac{1-\phi_{LRF}}{C_{HRF}+\frac{H_{HRF}}{4}} \cdot \frac{12C_{HRF}+H_{HRF}}{32} \cdot \frac{1}{1+\frac{Y_{N2,IVC}}{Y_{O2,IVC}}+\phi_{LRF} \cdot \frac{1}{C_{LRF}+\frac{H_{LRF}}{4}} \cdot \frac{12C_{LRF}+H_{LRF}}{32}}$$

(3)

Where ϕ_{LRF} and ϕ_{HRF} are the absolute equivalence ratios of low reactivity fuel and high reactivity fuel, C_{HRF} and C_{LRF} denote the number of carbon atoms, H_{HRF} and H_{LRF} are the number of hydrogen atoms, $Y_{N2,IVC}$ stands for nitrogen mass fraction at IVC and $Y_{O2,IVC}$ accounts the oxygen mass fraction at IVC.

Then, the model solves the general conservation equations either in a transient or steady formulation for axial momentum and fuel mass in terms of the on-axis (i.e., center line) referred to instantaneous values of velocity and species mass fractions. It is interesting to remark that the SoI_{HRF} and SoC timings obtained from the experimental work were used to provide the 1-D model calculation time for each test. Finally, by processing the raw results, the high reactivity fuel mass distribution mixed to different equivalence ratios at experimental SoC was obtained. Figure 3 shows an example of the 1-D model results as a histogram. In this case, the bars represent the result of the high reactivity fuel masses mixed to different local equivalence ratios and the solid line represents the envelope curve of the bars. For the sake of clarity, in the present work the results were also represented as a pie chart format.

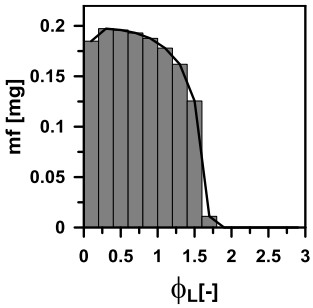

Figure 3. Histogram of the high reactivity fuel mass distribution mixed to different equivalence ratios at experimental SoC.

3. Test methodology

Previous works defined the in-cylinder fuel blending ratio (ICFB) as the low reactivity fuel mass versus the total fuel mass. However, since there is such a significant difference in LHV between E85 and the three remaining low reactivity fuels (Table 2), the premixed energy ratio (PER) is presented here. Thus, PER is defined as the energy ratio of the low reactivity fuel versus the total delivered energy:

$$\mathrm{PER}[\%] = \frac{\mathrm{m_{LRF}} \cdot \mathrm{LHV_{LRF}}}{\mathrm{m_{HRF}} \cdot \mathrm{LHV_{HRF}} + \mathrm{m_{LRF}} \cdot \mathrm{LHV_{LRF}}}$$

(4)

Where the subscripts LRF and HRF denote the low reactivity fuel and the high reactivity one, respectively.

In the present study, different PERs were tested depending on engine load. Moreover, for each specific PER, the total energy delivered to the cylinder was kept constant among the tests with the different fuel blends. In order to do this, the LRF mass was adjusted as required to compensate the differences in LHV, while the diesel injected mass was kept constant among the different blends. Figure 4, Figure 5 and Figure 6 show the different fuel mass, total energy delivered to the cylinder and global equivalence ratio for the different fuel blends at low, medium and high load. As noted from the figures, to reach the same total energy, a significantly higher E85 mass

amount is required compared to the remaining low reactivity fuels, overall when high PERs are proposed.

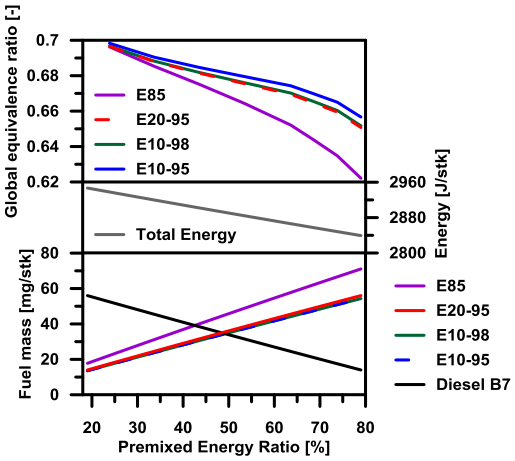

Figure 4. Testing conditions at low load. Fuel mass, total energy and global equivalence ratio for the different fuel blends versus PER.

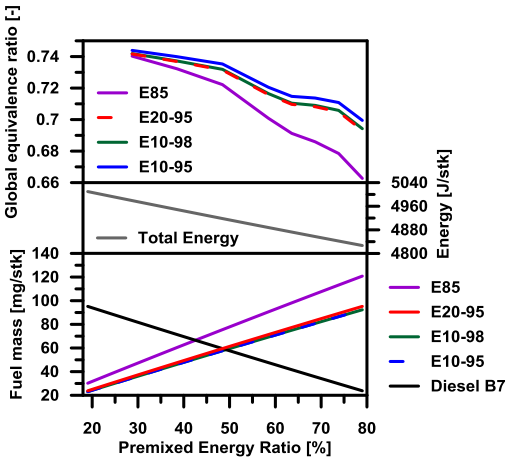

Figure 5. Testing conditions at medium load. Fuel mass, total energy and global equivalence ratio for the different fuel blends versus PER.

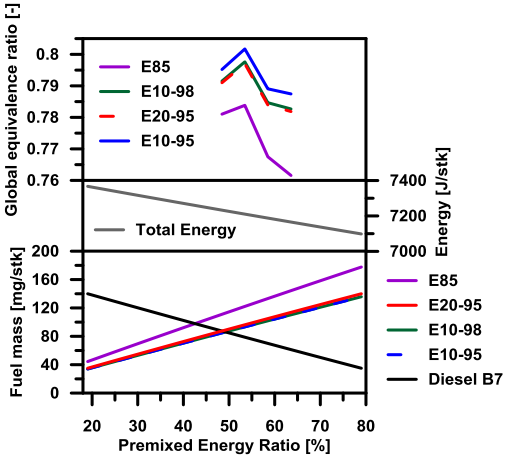

Figure 6. Testing conditions at high load. Fuel mass, total energy and global equivalence ratio for the different fuel blends versus PER.

4. Combustion development results

This section describes the effect of diesel injection timing, PER and fuel properties on combustion development at low, medium and high load. All the tests were carried out at fixed engine speed 1200 rpm, EGR 45% and intake temperature 40 °C. Table 5 depicts additional engine settings for the different engine loads.

Table 5. Constant engine settings for the different loads.

Load [-]	CR_{eff} [-]	HRF inj. strategy [-]	HRF inj. pressure [bar]	LRF inj. pressure [bar]	Intake pressure [bar]	Exhaust pressure [bar]
Low	14.4:1	Double	700	5.5	1.35	1.15
Medium	11:1	Double	800		2.96	2.76
High	11:1	Single	1890		3.4	3.2

In order to ensure moderated pressure rise rates to preserve the engine mechanical integrity at medium and high load, the effective compression ratio was lowered by means of advancing the intake valves closing event (early Miller cycle). For the same reason, a single injection strategy for the HRF was set at high load conditions.

4.1. Low load conditions

Table 6 depicts the diesel settings (SOI timing and fuel mass) as well as the fuel mass for the different LRFs and PERs at low load conditions. The shaded SOI_{main} values not enabled a stable combustion with any fuel blend. In particular, the excessive advance of the diesel SOI_{main} resulted in a too lean diesel distribution at SOC, which not allowed the combustion progression. This effect was more noticeable as PER was increased, where the limitation appeared even at more delayed SOI_{main}.

The HRF injection settings were selected focused on reaching EURO VI NOx and soot levels (discussed in section 5). In this sense, previous work developed at similar conditions [34] showed that the advanced diesel SOI_{pilot} at -60 CAD ATDC allows to

minimize NOx emissions while maintaining high efficiency and combustion stability. In addition, since the greater portion of the HRF (60% of the total diesel mass) had enough mixing time prior to SOC, soot formation was also reduced. On the other hand, the more delayed diesel SOI_{main} was set at -20 CAD ATDC to maintain CA50 near desired values.

The PERs tested in the case of B7+E85 were notably lower due to combustion stability issues. Specifically, tests with PER=54% resulted in a combustion development with a COV_{IMEP}>4.5% and CO and HC emission levels greater than 32 and 14 g/kWh, respectively. Thus, considering COV_{IMEP}=5% as an upper limit to attain a stable combustion, the highest PER proposed in the case of B7+E85 was 44% and the lower one 24%.

Table 6. Operating parameters at low load conditions. Diesel main injection timing sweep for the different fuel blends and premixed energy ratios.

Diesel SOI		Gasolines						E85			
Pilot [CAD]	Main [CAD]	$Diesel_{pilot}$ [mg]	$Diesel_{main}$ [mg]	PER [%]	E20-95 [mg]	E10-95 [mg]	E10-98 [mg]	$Diesel_{pilot}$ [mg]	$Diesel_{main}$ [mg]	PER [%]	E85 [mg]
-60	-20	14.7	9.8	64	45.5	44.1	44.1	31.5	21	24	22.2
	-25										
	-30										
	-35										
	-40										
	-20	12.6	8.4	69	49	47.5	47.5	27.3	18.2	34	31
	-25										
	-30										
	-35										
	-40										
	-20	10.5	7	74	52.5	50.9	50.9	232.1	15.4	44	40
	-25										
	-30										
	-35										
	-40										
	-20	8.4	5.6	79	56	54.3	54.3	19	12.7	54	48.9
	-25										
	-30										
	-35										
	-40										

Figure 7 shows the Influence of PER at low load in the case of advanced diesel SOI conditions (-60/-30 CAD). For the sake of clarity, only the RoHR traces corresponding to B7+E20-95 and B7+E85 are depicted. In this sense, the slight differences in properties among E20-95, E10-95 and E20-98, allows to perform the explanation based on B7+E20-95 (which has intermediate properties) and extrapolate it to the other two fuels. On the other hand, the specific RoHR traces of B7+E85 are also included due to its particular conditions.

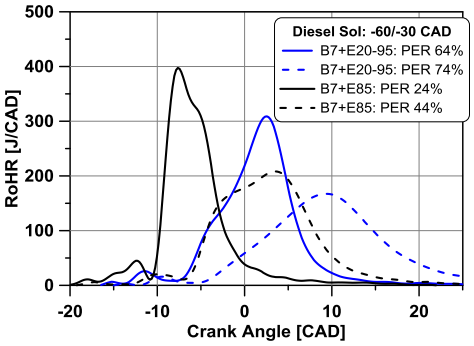

Figure 7. Influence of PER at low load with diesel injection timing at -60/-30 CAD. The RoHR traces of B7+E20-95 and B7+E85 are depicted.

Focusing on the effects of PER and fuel properties on RoHR shape, Figure 7 shows a one stage Gaussian-shaped heat release whatever the PER and fuel blend. This behavior is explained due to the highly advanced injection strategy of the HRF, which provides a well-mixed charge and then, a relatively fast heat release is attained when the proper thermodynamic conditions are reached. In the case of B7+E85 an appreciable change in the RoHR slope during the combustion development is observed. It is well related with the lower PER used as well as the higher differences in reactivity among the high and low reactivity fuels.

As literature demonstrates, in RCCI operation, the combustion starts with the autoignition of the HRF followed by the entrained LRF. The consequent increase in temperature and pressure initiates a flame propagation, which proceed gradually from

the high to the low reactivity regions of the combustion chamber [22][34]. In this work, the role of the blend reactivity on combustion progression can be examined comparing two different PERs for the same fuel blend. Thus, focusing on B7+E85 with PER=24%, a strong RoHR peak (due to the high amount of premixed diesel fuel mass) followed by a late soft burn (corresponding to the majority of E85 consumption) is appreciated. By contrast, PER=44% leads to a less pronounced RoHR slope at SOC. The different combustion pattern in this case is well related with the lower diesel amount injected combined with the higher mixing time, which results in a leaner local distribution at SOC (Figure 8). After the first instants, a soft RoHR is observed and finally another change in the RoHR slope is appreciated just after TDC, suggesting that the increase in temperature at the end of the compression stroke enhances the E85 consumption.

As a general conclusion, the increase in PER provides a reduction in the heat release peak as well as a delayed and larger combustion development. This behavior is explained due to the reduced in-cylinder global reactivity (i.e., higher RON of the mixture) as the LRF fraction in the mixture is increased. From Figure 7 is confirmed that this statement is also valid in the case of B7+E20-95.

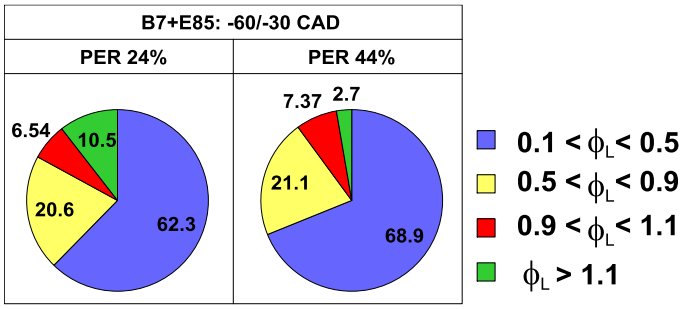

Figure 8. Effect of PER on mixing process at diesel injection timing of -60/-30 CAD. Equivalence ratio distribution at SOC for the cases of B7+E85 with PER 24% (left) and 44% (right).

As explained in the introduction section, RCCI concept allows a flexible operation by modifying both, the low reactivity fuel percentage in the blend and/or the direct

injection timing. Thus, an effective control of the combustion onset can be carried out. In this sense, Figure 7 presents an almost equal SOC of the HTHR stage when using B7+E20-95 with PER 64% and B7+E85 with PER 44%. Thus, the in-cylinder reactivity decrease due to the change in the LRF properties has been compensated by tuning the low to high reactivity fuel ratio in the blend. In spite of having similar SOC, the RoHR evolution denotes a very different combustion progression. This behavior is explained comparing the mixture distributions at SOC for this two cases (Figure 9). As Figure 9 shows, there is enough mixture in reactive conditions ($0.9<\phi<1.1$) to initiate the combustion for both fuel blends. Only a slightly higher percentage of mixture (1.86% greater) for B7+E85 in this range of equivalences ratios is observed. This difference is related with the lower mixing time for the diesel injection (longer injection rate and equal SOC) compared with the case of B7+E20-95. However, the lower mixture mixed to richer equivalence ratios ($\phi>1.1$) results in a softer and larger combustion propagation.

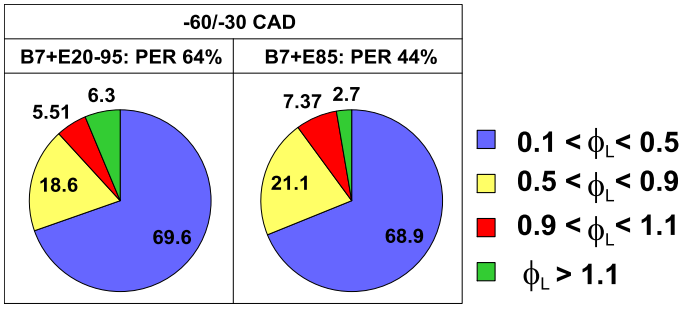

Figure 9. Mixing process differences among fuel blends with same experimental SOC. Equivalence ratio distribution at SOC for B7+E20-95 with PER 64% (left) and E85 with PER 44% (right) at diesel injection timing of -60/-30 CAD.

Figure 10 shows the most delayed injection timing achievable for all the fuel blends (-60/-20 CAD ATDC). In this case, a two staged heat release is observed for both fuel blends represented, whatever the PER used. This RoHR shape is attributed to the enhancement of the first premixed phase, which is mainly related with the diesel fuel

burned with a minimum amount of entrained low reactivity fuel. On the other hand, the increase in the PER provides the same effect that in the case of the advanced diesel SOI_{main} (-30 CAD ATDC). Thus, a soft RoHR with large combustion duration is attained for both fuel blends as PER is increased.

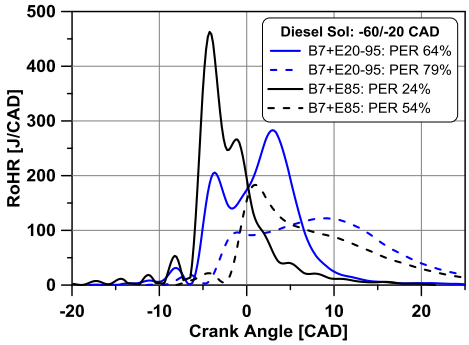

Figure 10. Influence of PER at low load for B7+E20-95 and B7+E85 at diesel injection timing of -60/-20 CAD.

To clarify the diesel SOI effect on RCCI combustion development, Figure 11 shows the RoHR traces of B7+E85 at two different SOIs, together with their mixture distribution at the experimental SOC. It is clear that the RoHR shape moves from a one stage Gaussian-shaped to a two staged heat release as the diesel SOI_{main} is moved from -30 to -20 CAD ATDC. This transition is associated with the lower extra mixing time (SOC-EOI) available as the diesel SOI_{main} is delayed, which provides a richer equivalence ratio distribution at SOC and enhances the premixed phase (higher maximum RoHR peak). By contrast, since a greater portion of the fuel has been already burned, the second RoHR peak becomes lower. It is interesting to note that the combustion duration (CA90-CA10) is almost constant as SOI_{main} is modified.

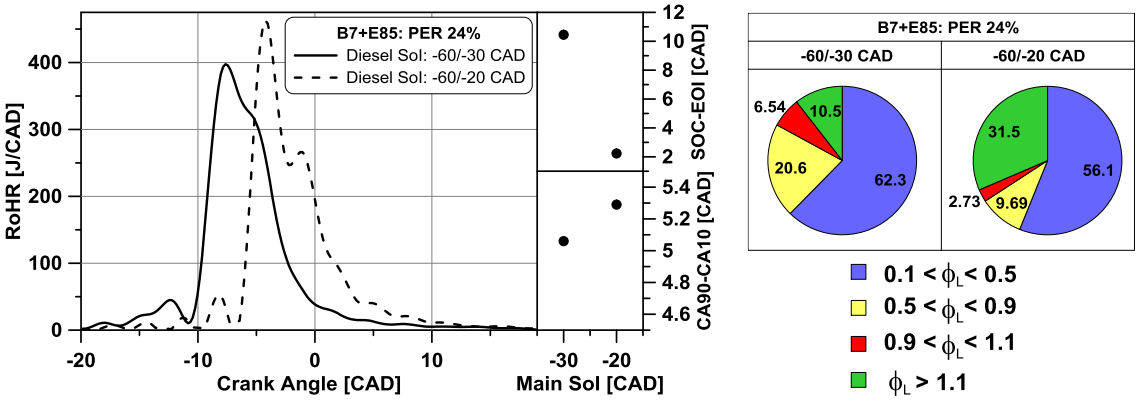

Figure 11. Effect of injection timing at low load. RoHR (left) and equivalence ratio distribution at SOC (right) for the cases of B7+E85 and PER 24% with diesel injection timing at -60/-30 and -60/-20 CAD.

Finally, in order to assess the specific differences among B7+E20-95, B7+E10-98 and B7+E10-95 in terms of combustion development, Figure 12 represents various combustion tracers for the tests depicted in Table 6. From the Figure, it is stated that an almost equal combustion development is attained for B7+E20-95 and B7+E10-98 whatever the PER and diesel SOI_{main}. In particular, almost equal combustion metrics with a minor differences in IMEP values are observed. These differences are mainly related to the very slight changes in CA50, CA90-CA10 and maximum RoHR peak. By contrast, B7+E10-95 allows shorter and advanced combustion development with higher maximum RoHR, leading to higher IMEP values. In this case, the ringing intensity is also increased but all the values are below 5 MW/m^2, which was established by Dec and Yang [35] as a proper upper limit to achieve an acceptable combustion noise and knock-free operation.

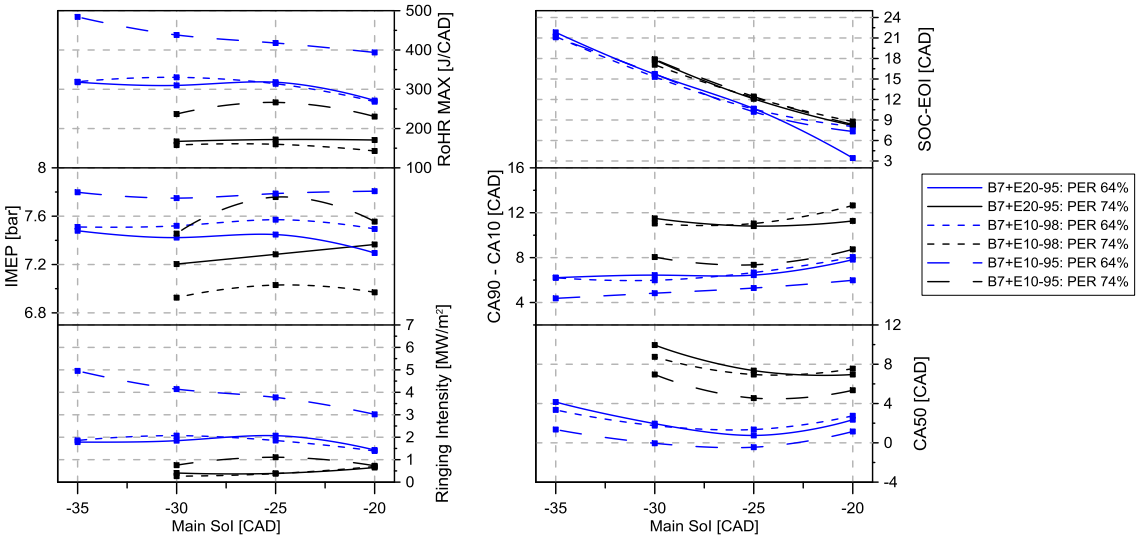

Figure 12. Combustion tracers of B7+E20-95, B7+E10-98 and B7+E10-95 blends at low load. Maximum RoHR, IMEP, ringing intensity, extra mixing time (SOC-EOI), combustion duration (CA90-CA10) and combustion phasing (CA50) are represented.

4.2. Medium load conditions

Table 7 depicts the operating parameters at medium load. The diesel SOI_{pilot} was also set at -60 CAD ATDC. It is interesting to remark that the PERs used in the case of B7+E85 were notably lower. As done at low load conditions, the highest PER operable was selected according to combustion stability criteria (COV_{IMEP}< 4.5%). The worst test with PER=49% resulted in a COV_{IMEP}=3.5% and CO and HC emission levels greater than 32 and 8 g/kWh, respectively. Thus, 49% was selected as the highest PER and the lower one proposed was 19%, as depicted in Table 7.

Table 7. Operating parameters at medium load conditions. Diesel main injection timing sweep for the different fuel blends and premixed energy ratios.

Diesel SOI		Gasolines						E85			
Pilot [CAD]	Main [CAD]	$Diesel_{pilot}$ [mg]	$Diesel_{main}$ [mg]	PER [%]	E20-95 [mg]	E10-95 [mg]	E10-98 [mg]	$Diesel_{pilot}$ [mg]	$Diesel_{main}$ [mg]	PER [%]	E85 [mg]
-60	-9	31.7	15.9	59	71.4	69.2	69.3	64	31.2	19	90.6
	-12										
	-15										
	-18										
	-21										
	-9	27.7	13.9	64	77.3	74.9	75	55.8	27.5	29	98.2
	-12										
	-15										
	-18										
	-21										
	-9	23.8	11.9	69	83.3	80.7	80.8	47.8	23.5	39	105.7
	-12										
	-15										
	-18										
	-21										
	-9	19.8	9.9	74	89.2	86.5	86.6	39.9	19.6	49	113.3
	-12										
	-15										
	-18										
	-21										

Figure 13 analyzes the effect of PER and fuel type on RoHR shape. For this purpose, the RoHR traces corresponding to the most advanced diesel SOI_{main} (-21 CAD ATDC) are presented. As previously done, B7+E20-95 has been selected as representative fuel blend of E10-95 and E10-98. In addition, RoHR traces of B7+E85 are also included in the figures due to its particular test conditions in terms of PER. Finally, a specific RoHR profile of B7+E10-95 is also depicted in the Figure.

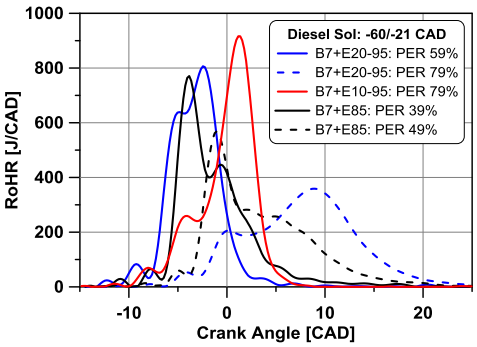

Figure 13. Influence of PER at medium load for B7+E20-95 and B7+E85 at diesel injection timing of -60/-21 CAD. A specific RoHR profile of B7+E10-95 has also included.

As seen from Figure 13, a two staged RoHR is obtained whatever the fuel and PER used. As a general trend a growth in the RoHR is observed after the first rapid ramp associated to the premixed combustion of diesel and the entrained LRF. On the other hand, B7+E85 exhibits the same behavior found at low load, with a first premixed RoHR peak followed by a softer combustion development. In addition, the increase in PER provides the same effect found in the previous section for both fuel blends.

In contrast to low load conditions, the LRF type has a considerable effect on RoHR combustion development for the same PER conditions. Thus, it should be noted the strong improvement in the second combustion stage that B7+E10-95 provides compared to B7+E20-95 fuel blend for the highest PER tested (79%). The higher reactivity of E10-95 results in more than double RoHR peak during the second combustion stage, when the majority of E10-95 is consumed, leading to combustion phasing 7.4 CAD advanced. It is interesting to note that the first RoHR peak for B7+E20-95 and B7+E10-95 is very similar, with slight differences associated to the lower mixing time available in the case of B7+E10-95. As seen in Figure 14, it results in a richer equivalence ratio distribution at SOC (higher fuel mass mixed between $1.1<\phi<2.3$).

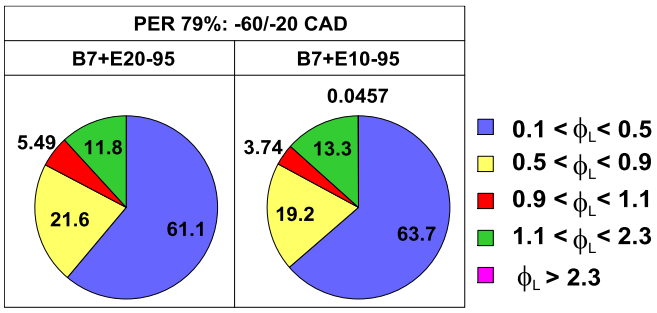

Figure 14. Equivalence ratio distribution at SOC for the cases of B7+E20-95 (left) and B7+E10-95 (right) with diesel injection timing at -60/-20 CAD and PER 79%.

From Figure 15 is stated that a diesel SOI_{main} set at -9 CAD results also in a two staged combustion development, but during the expansion stroke for all PERs and fuel blends. B7+E20-95 shows a first premixed phase followed by a second RoHR peak with similar J/CAD released than the first stage. Equal behavior is observed for both PERs. It should be noted that no difference in SOC is observed when PER is modified. In the particular case of B7+E85, a rapid ramp into HTHR is appreciated once the combustion started, followed by a diesel-like late combustion phase. Moreover, SOC is delayed 5.6 CAD when PER is increased from 19% to 29% with an almost equal maximum RoHR peak. Also of note is that equal SOC is obtained using E20-95 with PER 59% or PER 69% and E85 with PER 19%, with a higher RoHR peak in the last case due to the higher diesel amount and the shorter mixing time.

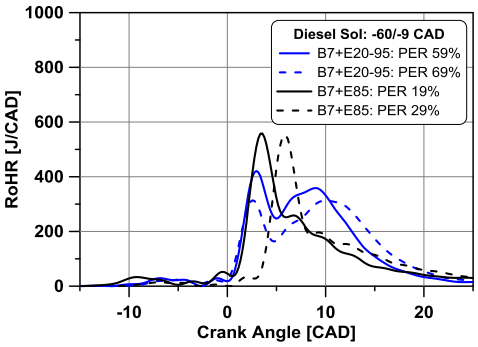

Figure 15. Influence of PER at medium load for B7+E20-95 and B7+E85 at diesel injection timing of -60/-9 CAD.

Figure 16 show the effect of diesel SOI on combustion behavior at medium load. For this purpose, the RoHR traces of B7+E20-95 at two timings of the main injection: -21 and -9 CAD ATDC are depicted. As Figure shows, both injection strategies lead to a two staged RoHR profile. However, the maximum RoHR moves from the second phase (in the case of -21 CAD) to the first phase (in the case of -9 CAD). In this sense, the lower extra mixing time (SOC-EOI) as SOI_{main} is delayed provides a richer equivalence ratio distribution at SOC, which enhances the reactions during the SOC. However, the higher

portion of mixture mixed to lean equivalence ratios (65.2%) when SOI_{main} is delayed together with the lower in-cyliner pressure and temperature during the expansion stroke, result in a smoother and larger combustion event. In the case of -21 CAD the increase in pressure and temperature during the first instants of the combustion promotes a powerful autoignition during the second RoHR slope.

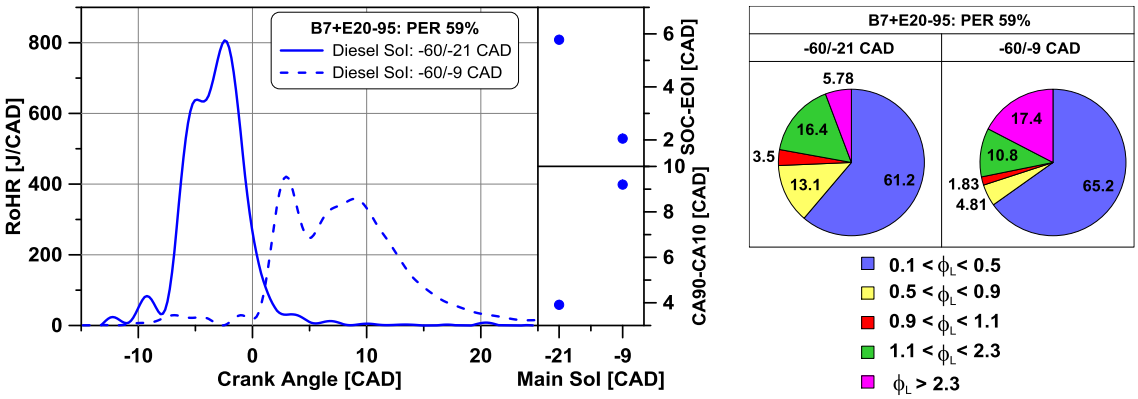

Figure 16. Effect of injection timing at medium load. RoHR (left) and equivalence ratio distribution at SOC (right) for the cases of B7+E20-95 and PER 59% with diesel injection timing at -60/-21 and -60/-9 CAD.

Figure 17 denotes greater differences in combustion development among fuel blends compared to low load conditions. However, the general trend with PER and SOI_{main} is nearly the same for all the fuel blends. Thus, a delayed diesel SOI_{main} provides larger and delayed combustion development, with shorter mixing time. In addition, lower maximum RoHR peak and RI are attained. Regarding B7+E10-95, it provides shorter and advanced combustion development with higher maximum RoHR compared to the remaining ones. IMEP values are very similar except for delayed diesel SOI_{main} timings, in which a drop is observed for B7+E20-95 and B7+E10-98. The improved reactivity of B7+E10-95 allows maintaining almost constant values at this point. Concerning ringing intensity, its values are clearly related with the blend reactivity (i.e., octane number). Specifically, values under 5 MW/m^2 are achieved using B7+E10-98 for all conditions tested. B7+E10-95 combustion leads to RI values greater than 5 MW/m^2 for the most

advanced SOI_{main} whatever the PER. Finally, B7+E20-95 exhibits an intermediate behavior, with low RI when using the highest PER and greater one when using advanced SOI_{main} combined with the lowest PER. These RI values do not compromise the engine mechanical integrity.

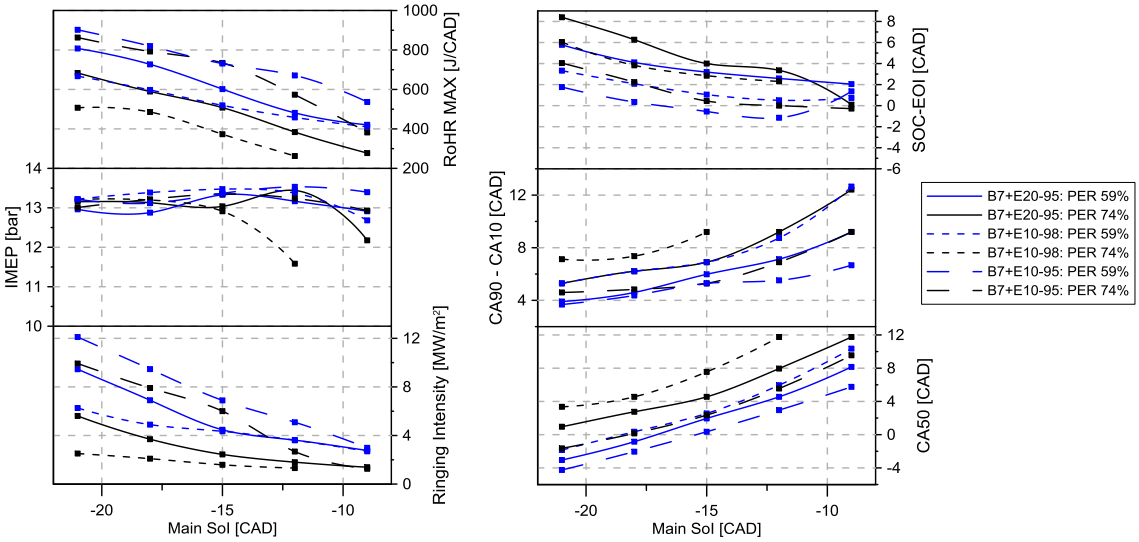

Figure 17. Combustion tracers of B7+E20-95, B7+E10-98 and B7+E10-95 blends at medium load. Maximum RoHR, IMEP, ringing intensity, extra mixing time (SOC-EOI), combustion duration (CA90-CA10) and combustion phasing (CA50) are represented.

4.3. High load conditions

Table 8 depicts the different operating parameters proposed for the tests at high load. In this case, PER values were the same for all the fuel blends, including B7+E85. It is interesting to remark the extremely narrow operating range found when using B7+E85. In particular, only two tests were possible to carry out, the ones corresponding to diesel SOI set at -6 and -3 CAD ATDC with the lowest PER (49%). Diesel injection timings more delayed than -3 CAD ATDC resulted in misfire and diesel injection timings more advanced than -6 CAD ATDC resulting in excessive knocking level. Moreover, PERs lower than 49% resulted in excessive knocking level due to the greater diesel mass burned during the premixed stage and PERs higher than 49% were not possible to test due to valve pooling. In this sense, the low LHV of E85 made necessary larger

injection durations to provide the same energy to the cylinder. This fact combined with the advance in the intake valves closing event resulted in the cycle-to-cycle injected mass variation, endangering the mechanical integrity of the engine when great amount of ethanol was accumulated and burned.

Table 8. Operating parameters at high load conditions. Diesel injection timing sweep for the different fuel blends and premixed energy ratios.

Diesel SOI [CAD]	Diesel [mg]	PER [%]	E20-95 [mg]	E10-95 [mg]	E10-98 [mg]	E85 [mg]
-9	87.5	49	87.5	84.8	84.9	111
-6						
-3						
0						
3						
6						
-9	78.7	54	78.7	93.3	93.4	122.1
-6						
-3						
0						
3						
6						
-9	70	59	70	101.8	101.8	133.2
-6						
-3						
0						
3						
6						
-9	61.2	64	61.2	110.2	110.3	144.3
-6						
-3						
0						
3						
6						

Figure 18 presents the effect of PER on combustion pattern at the most advanced diesel SOI timing reached with all the fuels. As it is seen from the figure, the combustion trace of B7+E20-95 with the highest PER shows a double staged RoHR with an almost equal peaks among the two combustion phases. In this case, the reduction in PER not affect the first combustion stage, while the second one is clearly worsened.

Moreover, a slower combustion development with an intermediate RoHR peak is observed when PER is reduced, which suggest an inappropriate equivalence ratio stratification in the combustion chamber. Thus, unlike at low and medium load conditions, the increase in PER enhances the combustion development.

The direct comparison of both fuel blends (B7+E20-95 vs B7+E85) for the same PER and SOI conditions reveals a delay in SOC of around 2.5 CAD in the case of B7+E85. It should be related to the lower reactivity of E85 as well as its higher heat of vaporization than E20-95 fuel. In spite of that, a stronger rise in the RoHR slope is appreciated once the combustion has started. It is explained due to the higher mixture amount mixed in the range of (1.1<ϕ<2.3). On the other hand, both fuel blends exhibit a late combustion phase. The only difference is the slight growth in the RoHR with B7+E20-95, probably because of its richer mixture distribution (ϕ >2.3).

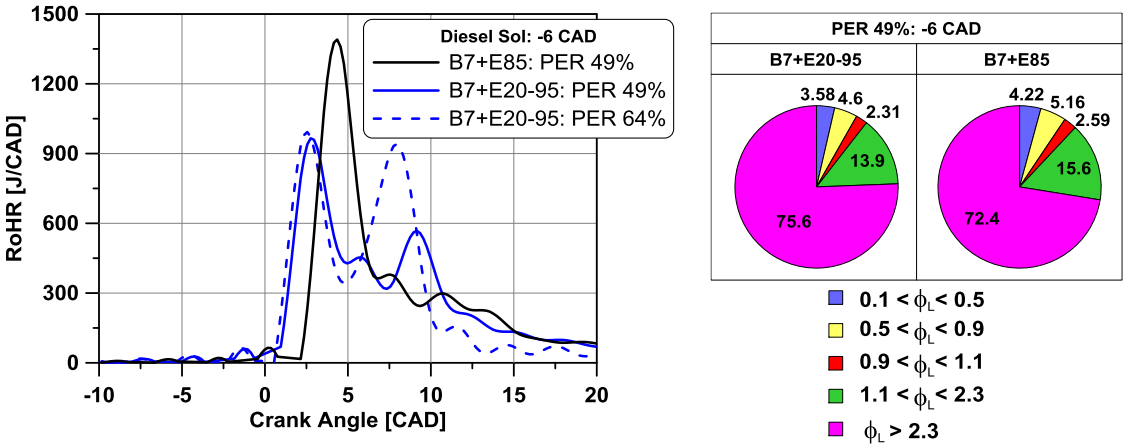

Figure 18. Influence of PER at high load for B7+E20-95 and B7+E85 at diesel injection timing of -6 CAD.

Figure 19 shows a very late combustion development for the case of diesel SOI set at +3 CAD ATDC (delayed scenario). At this condition, no remarkable effect of PER on SOC and combustion duration is appreciated. The combustion shape is the same that the one described for B7+E85 at -6 CAD ATDC. In addition, slightly higher RoHR is appreciated for the lower PER, due to the higher diesel amount injected.

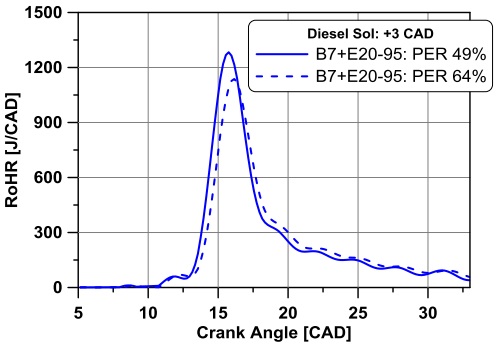

Figure 19. Influence of PER at high load for B7+E20-95. RoHR traces at diesel injection timing of +3 CAD with PER 49% and 64% are represented.

Figure 20 presents the effect of injection timing on combustion behavior at high load. For this purpose, the RoHR traces of B7+E20-95 at two diesel SOIs (-6 and +3 CAD ATDC) for the same PER (49%) are depicted. As seen in the figure, the RoHR shape changes from two to one stage. The mixture distribution analysis reveals a very similar mixture at SOC in both cases. Thus, the thermodynamic conditions (pressure and temperature) govern this change in the RoHR shape. The first RoHR peak, which is associated to the mixture amount mixed to the reactive equivalence ratios ($1.1<\phi<2.3$), is very similar in both cases. However, even having enough mixture in rich equivalence ratio conditions ($\phi>2.3$), the low temperature associated to the expansion stroke avoids to propagate a second phase in the case of +3 CAD ATDC.

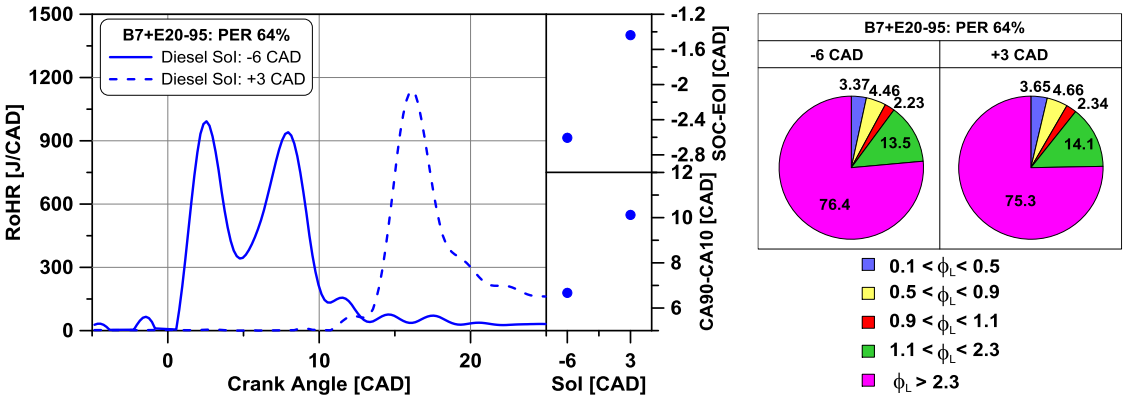

Figure 20. Effect of injection timing at high load. RoHR (left) and equivalence ratio distribution at SOC (right) for the cases of B7+E20-95 and PER 64% with diesel injection timing at -6 and +3 CAD.

Figure 21 illustrates various combustion tracers to compare the combustion development among B7+E20-95, B7+E10-98 and B7+E10-95 for all the tests depicted in Table 8. As found at low and medium loads, the higher reactivity of E10-95 results in shorter combustion duration and advanced SOC compared to the other LRFs. It is also interesting to remark that E10-95 allows the combustion propagation even when an extremely delayed SOI_{main} is proposed (+6 CAD TDC), in which misfire is observed for the other fuel blends. Concerning combustion phasing (CA50), very similar values are attained for all the fuel blends, which denotes the combustion development is mainly governed by the diesel injection. Regarding IMEP, values almost collide for all the fuel blends, with slight differences associated to the combustion duration and maximum RoHR. Finally, no clear trend is observed in terms of ringing intensity. All the values are confined between 12 and 15 MW/m^2 for B7+E20-95 and B7+E10-98 and a unacceptable RI value around 25MW/m^2 is registered for B7+E10-95 at -9 CAD ATDC with the highest PER (64%).

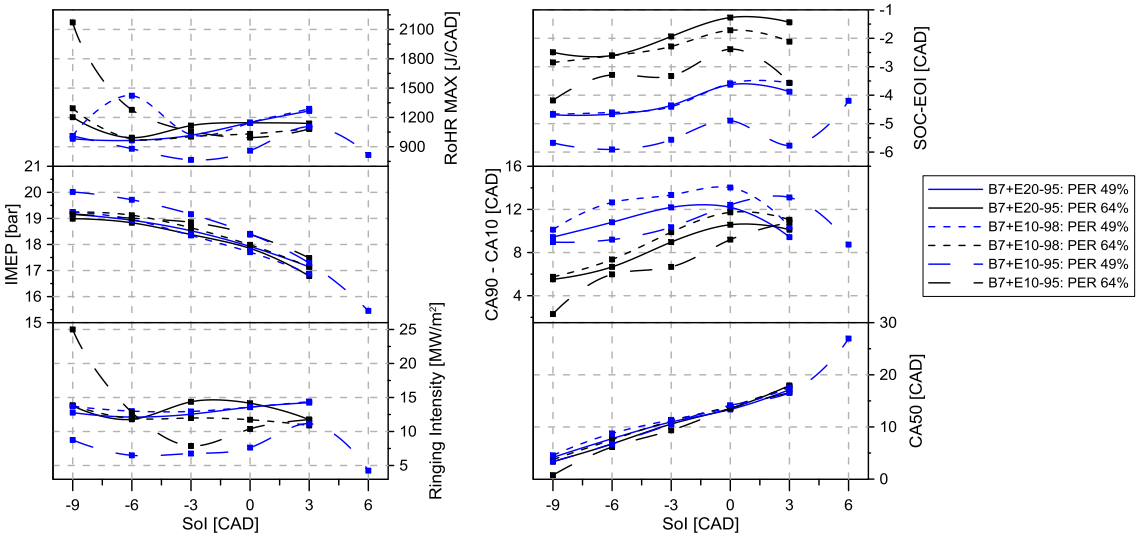

Figure 21. Combustion tracers of B7+E20-95, B7+E10-98 and B7+E10-95 blends at high load. Maximum RoHR, IMEP, ringing intensity, extra mixing time (SOC-EOI), combustion duration (CA90-CA10) and combustion phasing (CA50) are represented.

5. Performance and engine-out emissions results

5.1. NOx emissions

Figure 22 represents the NOx emissions for the different PERs and blends at the different loads. Dashed lines across the figures denote the EURO VI NOx limits for HD diesel engines (NOx <0.4 g/kWh). It is stated that B7+E20-95, B7+E10-98 and B7+E10-95 blends show the same general trend with respect to diesel SOI and PER variations at different engine loads. Only specific differences are identified at certain operating conditions. On the other hand, B7+E85 blend exhibits a similar trend with very different values.

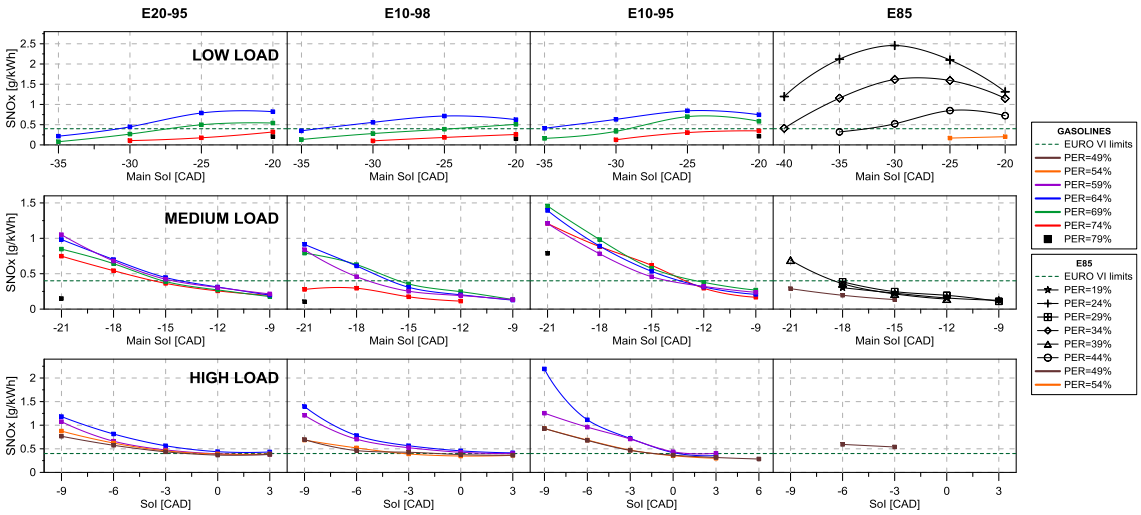

Figure 22. NOx emissions for the different premixed energy ratios and fuel blends at low, medium and high load.

At low load, a delay in diesel SOI_{main} as well as a reduction in PER result in a NOx emissions increase whatever the fuel blend. This trend is explained focusing on the results presented in Figure 7. From Figure 7 it is demonstrated that, at low load, a reduction in PER enhances the combustion process leading to higher maximum RoHR peaks. On the other hand, it is also confirmed that CA50 is shifted to high temperature instants in the cycle as diesel SOI_{main} is delayed. Both effects directly contributes to

increase the NOx emissions. In the case of B7+E85, diesel SOIs delayed from -30 CAD ATDC result in a poor combustion, reducing NOx emissions. Moreover, as seen in Section 4.1, the lower PERs used to maintain a stable combustion with B7+E85 promote stronger RoHR peaks (due to the high amount of premixed diesel fuel mass) which explains the higher NOx levels registered for the same SOI. Also of note is that EURO VI limits are achieved for E20-95, E10-98 and E10-95 with the highest PER (74%), whatever the diesel SOI.

At medium load, the effect of PER is only noticeable for advanced diesel SOIs, with higher NOx levels as PER is reduced. By contrast, injection timing effect is opposite to the one observed at low load because of the range tested. From Figure 16 it is stated that SOI_{main} delayed from -21 CAD results in a combustion development during expansion stroke with a soft RoHR evolution, which contributes to reduce NOx emissions. It is interesting to remark the strong improvement in NOx emissions achieved using B7+E85 at this load. Almost all the tests leads to NOx values under EURO VI limitation.

Finally, at high load, the injection timing effect on NOx emissions is similar to the one observed at medium load, but the effect of PER is opposite. As shown in Figure 18, at high load, the combustion development is clearly improved as PER is increased. This fact promotes higher combustion temperatures and therefore higher NOx emissions. As at medium load conditions, EURO VI limits are only fulfilled for the more delayed SOIs. Finally, NOx emissions for E10-95 are higher than E20-95 and E10-98 whatever the engine load due to the improved reactivity.

5.2. Soot emissions

Soot emissions for the different premixed energy ratios and blends at low, medium and high load are shown in Figure 23. Dashed lines across the figures denote the EURO VI soot limits for HD diesel engines (soot <0.01 g/kWh).

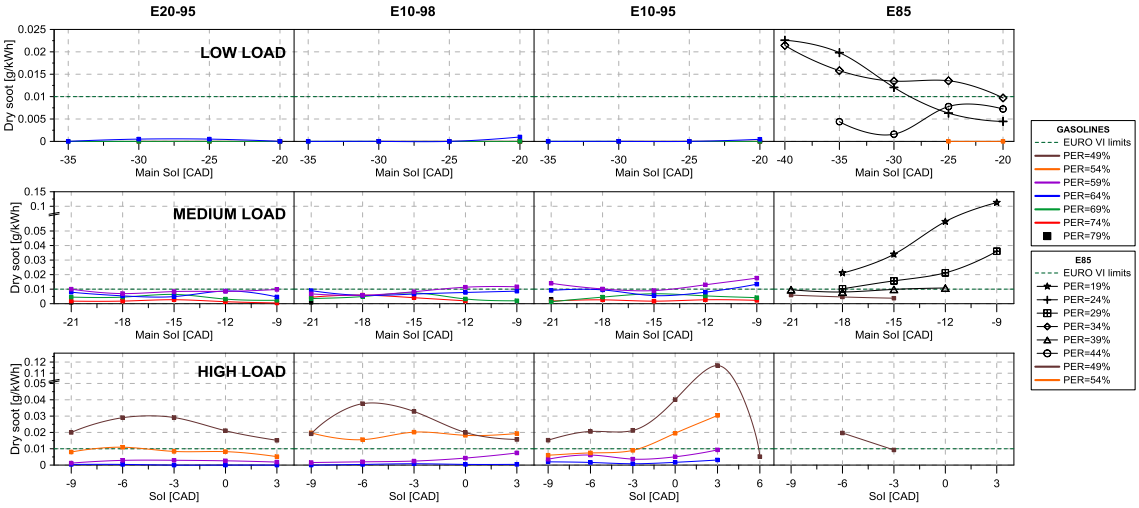

Figure 23. Soot emissions for the different premixed energy ratios and fuel blends at low, medium and high load.

At low load, soot levels registered are below the minimum detection limit of the AVL 415S Smoke Meter in all tests for B7+E20-95, B7+E10-98 and B7+E10-95. Thus, it is stated that an advanced enough injection strategy for the direct injected fuel provides sufficient mixing time prior to the start of combustion to inhibit soot formation.

B7+E85 fuel blend exhibits a different behavior. In this case, the higher PERs tested not allow to inhibit soot formation even using an advanced injection strategy for the high reactivity fuel. In general, as PER is decreased, soot emissions are increased due to the higher diesel amount in the blend. In addition, as SOI_{main} is delayed soot levels are lowered, due to the improvement in soot oxidation.

At medium load, soot values greater than zero are registered and consequently the effect of PER is more noticeable. In particular, higher soot levels are obtained as the diesel fuel mass is increased (lower PER). The diesel main injection timing has not a

strong effect on soot emissions. Only the most delayed SOIs for the lowest PERs presents values above the EURO VI limits. At this injection timing, the combustion development is shifted to the expansion stroke, which worsens the soot oxidation. Regarding B7+E85, EURO VI limits are fulfilled for PER 39% and 49% whatever the SOI_{main}. As PER is decreased unacceptable values are attained, mainly for the lowest PER (19%). As in the case of the other blends, the delay in SOI_{main} shifts the combustion to the expansion stroke worsening soot oxidation process.

At high load, the effect of PER is very noticeable. Thus, higher soot levels are registered as PER is decreased. As demonstrated in Figure 21, part of the diesel fuel is burned as diffusion flame (negative SOC-EOI) and therefore high soot levels are promoted. The differences in soot values among B7+E20-95, B7+E10-98 and B7+E10-95 are well related with their differences in extra mixing time. This fact is clear focusing on B7+E10-95 results, in which unacceptable soot levels are obtained for diesel SOI_{main} more delayed than -3 CAD ATDC and PER 49%. It is also interesting to note that B7+E20-95 provides values under EURO VI limits even using PER 54%. In addition, B7+E85 leads to improved results than the other fuel blends for the same PER (49%).

5.3. HC and CO emissions

Figure 24 and Figure 25 represent HC and CO emissions for the different premixed energy ratios and blends at low, medium and high load. Dashed lines across the figures denote the EURO VI HC and CO limits for HD diesel engines (HC <0.13 g/kWh and CO <1.5 g/kWh).

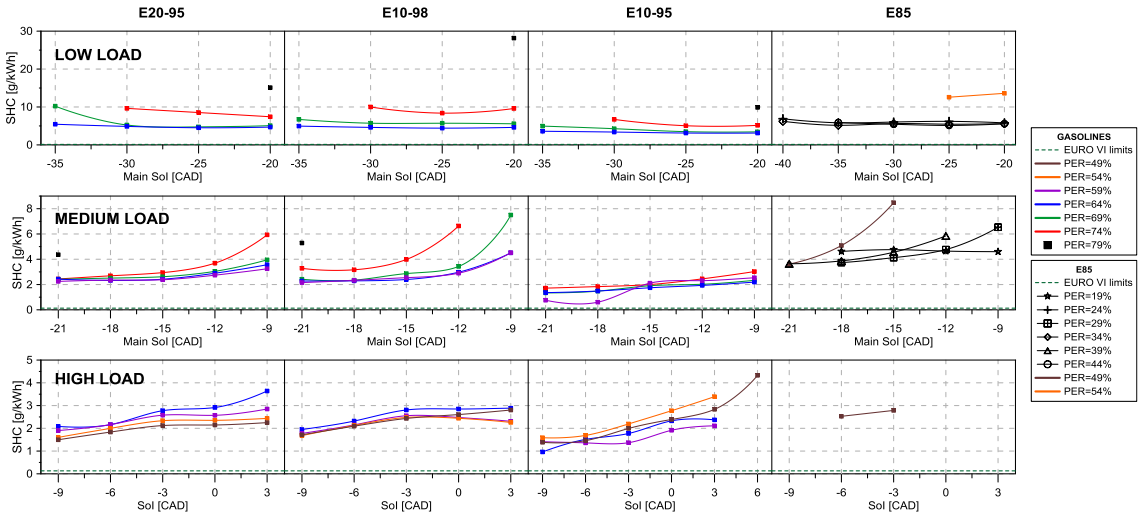

Figure 24. HC emissions for the different premixed energy ratios and fuel blends at low, medium and high load.

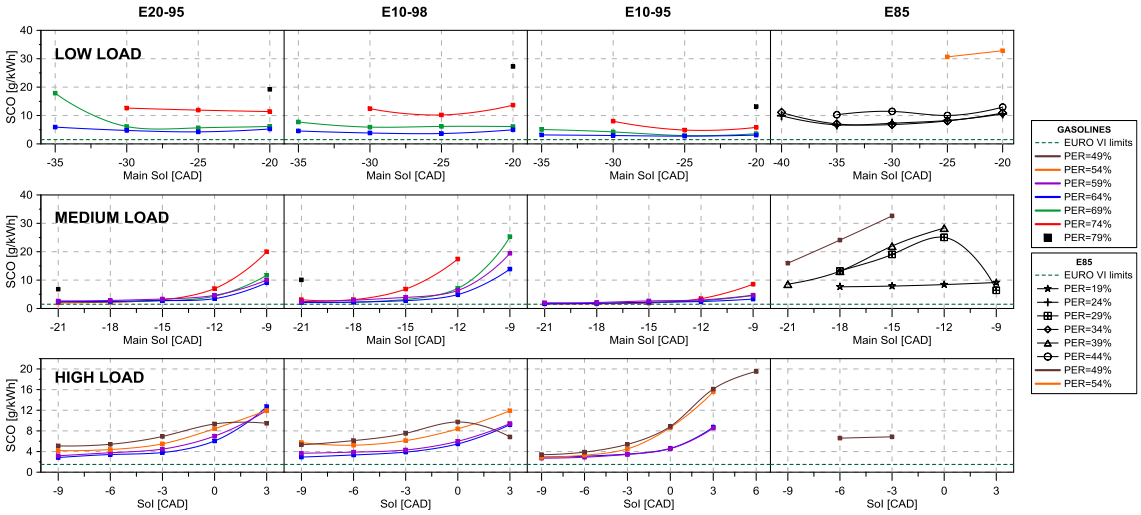

Figure 25. CO emissions for the different premixed energy ratios and fuel blends at low, medium and high load.

Focusing on low load results, no appreciable effect of diesel SOI_{main} on HC and CO emissions is observed. Previous studies combining computational and experimental results [34] demonstrated that unburned HC emissions from RCCI combustion at low load strongly depend on geometric parameters such as crevices and squish volumes, without a notable dependency with the engine settings. By contrast, CO emissions presented greater dependency to the engine settings because of the modification in the combustion temperature. In this case, the combustion metrics presented in Figure

12 remain almost constant as SOI_{main} is modified, without having a relevant effect on CO oxidation. The PER modification has the same effect on HC and CO emissions. As demonstrated in previous sections, at low load, an increase in PER results in a worsened combustion process leading to higher HC and CO emissions. The effect of SOI_{main} on HC and CO emissions at medium and high load is equal. Delayed injection timings result in a poor combustion development during the expansion stroke, and therefore higher emission levels are attained. The effect of PER on HC and CO emissions at medium load is equal to the one described at low load conditions. At high load the effect is opposite. As explained, as PER is increased, the combustion development is improved in this case.

6. General discussion

A merit function [36] was used to select the proper engine settings for the different fuel blends and engine loads. The values of the self-imposed constraints used to calculate the merit function were NOx=0.4 g/kWh, soot=0.01 g/kWh and PRR=15 bar/CAD. These limitations were aimed to fulfill EURO VI limits while preserving the engine mechanical integrity. Thus, the contribution to the merit function from a given variable will be zero if only the measured value is less than or equal to the specified limit. When F is non-zero, the contribution from each constrained parameter can be examined separately to quantify the severity of its non-compliance. The merit function is defined as follows:

$$F = \sum_i \max\left(0, \frac{x_i}{x_i^*} - 1\right) \quad (5)$$

If various operating conditions fulfilled all the constraints (which results in a merit function value of zero) for the same fuel blend and load, the best condition was considered the one that minimized the CO and HC emission levels.

Figure 26 shows the merit function results for all the tests carried out in this work. In addition, the selected engine operating conditions together with their merit function value are also marked in the figure. As seen from the figure, the selected operating conditions with the exception of E85 at high load, fulfilled all the constraints.

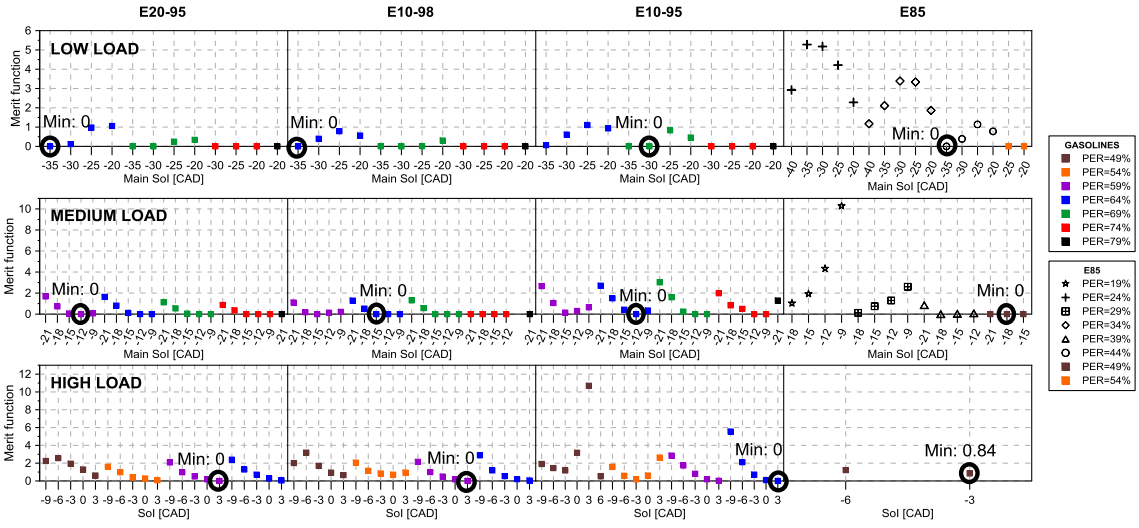

Figure 26. Merit function results calculated taking into account three self-imposed constraints: NOx <0.4 g/kWh, soot <0.01 g/kWh and maximum PRR <15 bar/CAD. The remarked operating conditions correspond to the ones that provide minimum CO and HC emission levels.

To summarize these results, Figure 27 represents NOx, soot, maximum PRR and combustion efficiency versus the engine load for the tests previously selected. As seen from the figure, EURO VI soot levels are reached whatever the fuel blend and engine load. Moreover, B7+E20-95, B7+E10-98 and B7+E10-95 lead also to NOx emissions under EURO VI limits for all the engine loads. By contrast, B7+E85 exceeds the limitation due to lower PER required to ensure stable operation. On the other hand, the maximum PRR remains below the self-imposed restriction for B7+E20-95, B7+E10-98 and B7+E10-95, while B7+E85 leads to an unacceptable values at high load. Finally,

it is interesting to remark that E10-95 improves the combustion efficiency at low and medium load, with similar values than E10-98 at high load.

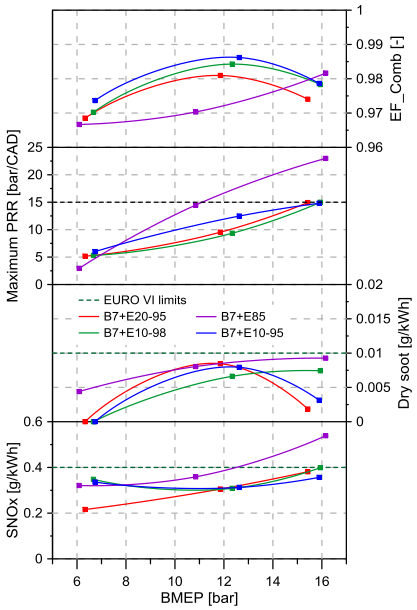

Figure 27. NOx, soot, maximum PRR and combustion efficiency versus engine load for the selected engine operating conditions.

7. Conclusions

In the present work, the influence of the direct injection timing and blending ratio on RCCI combustion have been studied by combining theoretical and experimental tools. Thus, an analysis of the parameters derived from the in-cylinder pressure measurement has been complemented with a detailed study of the air/fuel mixing process by means of a 1-D spray model. The major findings from the combustion development study at the different engine loads are summarized as follows:

- For all the engine loads, B7+E20-95, B7+E10-98 and B7+E10-95 exhibited similar combustion behavior when diesel SOI_{main} was modified. Thus, a delay in diesel SOI_{main} enhanced the premixed phase leading to a two staged heat release.

- Regarding the effect of SOI_{main} on RoHR shape, an advanced injection timing resulted in a one stage Gaussian-shaped heat release at low load. By contrast, a delayed diesel injection timing provided a two staged heat release. The greater diesel mass injected at medium and high load enhanced the premixed phase, leading to a two staged heat release either with an advanced or delayed diesel SOI.
- The increase in the PER resulted in lower heat release peaks with larger combustion developments at low and medium load. By contrast, at high load, the combustion development was clearly improved as PER was increased.
- The improved reactivity of E10-95 led to shorter and advanced combustion development for all the engine loads. These facts combined with higher maximum RoHR peaks, promoted higher IMEP values.
- The physicochemical properties of E85 resulted in a particular combustion behavior. Thus, lower PERs were required to achieve a stable combustion at low and medium load. On the other hand, an extremely narrow operating range was found at high load. In this sense, a slight advancing in diesel SOI around the stable operating point resulted in excessive knocking level while a slight delaying provoked misfire conditions.
- Finally, the required greater diesel amount with E85 led to a specific combustion development for all the engine loads. In particular, a strong rise in the first RoHR slope followed by a diesel-like tail was observed.

The notable observations comparing the performance and engine-out emissions from the different combinations of high and low reactivity fuel were as follows:

- NOx emissions are well related to the combustion temperatures. Thus, diesel SOI timings that provides combustion phasing near TDC promote an increase in NOx levels. The effect of PER is the same for all the fuel blends but depends on the engine load. At low and medium loads, the increase in PER worsens the combustion process resulting in lower NOx emissions. At high load, an opposite behavior is confirmed.
- An advanced injection strategy for the high reactivity fuel allows to inhibit soot formation at low load. At medium and high load, soot emissions are governed by formation/oxidation processes with higher values registered as PER is decreased. Moreover, unacceptable soot levels are registered for B7+E85 at low load.
- At low and medium load, an increase in PER results in a worsened combustion process leading to higher HC and CO emissions. At high load, the effect is the opposite. On the other hand, at low and medium loads the diesel SOI_{main} has no appreciable effect on HC and CO. Only a strong rise in the emissions is appreciated for delayed injection timings (when the combustion is degraded). In the case of high load, the single injection strategy proposed governs the combustion process, and therefore, the diesel SOI effect is more appreciable.

Finally, the results presented in this paper show that RCCI operation in a heavy-duty diesel engine with B7+E20-95, B7+E10-98 and B7+E10-95 allows fulfilling EUROVI NOx and soot emission levels with acceptable ringing intensity values at low, medium and high load. In addition, the higher reactivity of B7+E10-95 blend provides improved combustion efficiency.

Acknowledgments

The authors acknowledge VOLVO Group Trucks Technology and TOTAL for supporting this research.

References

[1]Kimura S, Aoki O, Kitahara Y, Aiyoshizawa E. Ultra-Clean Combustion Technology Combining a Low- Temperature and Premixed Combustion Concept for Meeting Future Emission Standards. SAE Technical Paper 2001-01-0200, 2001, doi:10.4271/2001-01-0200.

[2]Yanagihara H, Sato Y, Minuta J. A simultaneous reduction in NOx and soot in diesel engines under a new combustion system (Uniform Bulky Combustion System e UNIBUS). 17th International Vienna Motor Symposium, pp. 303-314, 1996.

[3]Mingfa Y, Zhaolei Z, Haifeng L. Progress and recent trends in homogeneous charge compression ignition (HCCI) engines. Progress in Energy and Combustion Science 35 (5) (October 2009) 398-437.

[4]Cerit M, Soyhan H S. Thermal analysis of a combustion chamber surrounded by deposits in an HCCI engine. Applied Thermal Engineering 50 (1) (2013) 81-88.

[5]Bessonette P W, Schleyer C H, Duffy K P, Hardy W L, Liechty M P. Effects of fuel property changes on heavy-duty HCCI combustion. SAE paper 2007-01-0191, 2007.

[6]Kalghatgi G, Risberg P, Ångström H. Partially Pre-Mixed Auto-Ignition of Gasoline to Attain Low Smoke and Low NOx at High Load in a Compression Ignition Engine and Comparison with a Diesel Fuel. SAE Technical Paper 2007-01-0006, 2007, doi:10.4271/2007-01-0006.

[7]Hanson R, Splitter D, Reitz R. Operating a Heavy-Duty Direct-Injection Compression-Ignition Engine with Gasoline for Low Emissions. SAE Technical Paper 2009-01-1442, 2009, doi:10.4271/2009-01-1442.

[8]Kalghatgi G, Risberg P, Angstrom H. Advantages of fuels with high resistance to autoignition in late-injection, low-temperature, compression ignition combustion. SAE Trans., 2006, 115(4), 623–634.

[9]Lewander C M, Johansson B, Tunestal P. Extending the Operating Region of Multi-Cylinder Partially Premixed Combustion using High Octane Number Fuel. SAE Paper 2011-01-1394; 2011.

[10]Liu H, Yao M, Zhang B, Zheng Z. Effects of inlet pressure and octane numbers on combustion and emissions of a homogeneous charge compression ignition (HCCI) engine. Energy and Fuels, 2008, 22(4), 2207–2215.

[11]Christensen M, Hultqvist A, Johansson B. Demonstrating the multi-fuel capability of a homogeneous charge compression ignition engine with variable compression ratio. SAE paper 1999-01-3679, 1999.

[12]Benajes J, García A, Domenech V, Durrett R. An investigation of partially premixed compression ignition combustion using gasoline and spark assistance. Applied Thermal Engineering, Volume 52, Issue 2, 15 April 2013, Pages 468-477.

[13]Pastor JV, García-Oliver JM, García A, Micó C, Durrett R. A spectroscopy study of gasoline partially 365 premixed compression ignition spark assisted combustion. Applied Energy 2013;104:568–75. 366.

[14]Benajes J, García A, Tormos B, Monsalve-Serrano J. Impact of Spark Assistance and Multiple Injections on Gasoline PPC Light Load. SAE Int. J. Engines 7(4):2014, doi:10.4271/2014-01-2669.

[15]Desantes JM, Payri R, García A, Monsalve Serrano J. Evaluation of Emissions and Performances from Partially Premixed Compression Ignition Combustion using

Gasoline and Spark Assistance. SAE Technical Paper 2013-01-1664, 2013, doi:10.4271/2013-01-1664.

[16]Benajes J, Molina S, García A, Monsalve-Serrano J, Durrett R. Conceptual model description of the double injection strategy applied to the gasoline partially premixed compression ignition combustion concept with spark assistance. Applied Energy, Volume 129, 15 September 2014, Pages 1-9.

[17]Benajes J, Molina S, García A, Monsalve-Serrano J, Durrett R. Performance and engine-out emissions evaluation of the double injection strategy applied to the gasoline partially premixed compression ignition spark assisted combustion concept. Applied Energy, Volume 134, 1 December 2014, Pages 90-101.

[18]Splitter D A, Wissink M L, Hendricks T L, Ghandhi J B, Reitz R D. Comparison of RCCI, HCCI, and CDC Operation from Low to Full Load, THIESEL 2012 Conference on Thermo- and Fluid Dynamic Processes in Direct Injection Engines, 2012.

[19]Splitter D A, Reitz R. Fuel reactivity effects on the efficiency and operational window of dual-fuel compression ignition engines. Fuel, Volume 118, 15 February 2014, Pages 163-175.

[20]Li J, Yang W M, An H, Zhou D Z, Yu W B, Wang J X, Li L. Numerical investigation on the effect of reactivity gradient in an RCCI engine fueled with gasoline and diesel. Energy Conversion and Management, Volume 92, 1 March 2015, Pages 342-352.

[21]Zhou D Z, Yang W M, An H, Li J, Shu C. A numerical study on RCCI engine fueled by biodiesel/methanol. Energy Conversion and Management, Volume 89, 1 January 2015, Pages 798-807.

[22]Kokjohn S L, Hanson R M, Splitter D A, Reitz R D. Fuel reactivity controlled compression ignition (RCCI): a pathway to controlled high-efficiency clean combustion, International Journal of Engine Research, 2011. Volume 12, June 2011, Pages 209-226.

[23]Splitter D A, Kokjohn S L, Wissink M L, Reitz R. Effect of compression ratio and piston geometry on RCCI load limits and efficiency. SAE technical paper 2012-01-0383; 2012. http://dx.doi.org/10.4271/2012-01-0383.

[24]Tutak W. Bioethanol E85 as a fuel for dual fuel diesel engine. Energy Conversion and Management, Volume 86, October 2014, Pages 39-48.

[25]Şahina Z, Durguna O, Mustafa Kurtb M. Experimental investigation of improving diesel combustion and engine performance by ethanol fumigation-heat release and flammability analysis. Energy Conversion and Management, Volume 89, 1 January 2015, Pages 175–187.

[26] Sarjovaara T, Alantie J, Larmi M. Ethanol dual-fuel combustion concept on heavy duty engine. Energy, Volume 63, 2013, Pages 76-85.

[27] Sarjovaara T, Larmi M. Dual fuel diesel combustion with an E85 ethanol/gasoline blend. Fuel, Volume 139, 2015, Pages 704-714.

[28]Payri F, Olmeda P, Martín J, García A. A complete 0D thermodynamic predictive model for direct injection diesel engines. Applied Energy, Volume 88, Issue 12, December 2011, Pages 4632-4641.

[29]Payri F, Olmeda P, Martin J, Carreño R. A New Tool to Perform Global Energy Balances in DI Diesel Engines. SAE Int. J. Engines 7(1):2014, doi:10.4271/2014-01-0665.

[30]Eng J. Characterization of pressure waves in HCCI combustion. SAE paper 2002-01-2859, 2002.

[31]Arrègle J, López JJ, García JM, Fenollosa C. Development of a zero-dimensional diesel combustion model, part 2: analysis of the transient initial and final diffusion combustion phases. Applied Thermal Engineering, 23 (2003) 1319e1331.

[32]Pastor JV, López JJ, García JM, Pastor JM. A 1D model for the description of mixing-controlled inert diesel sprays. Fuel 87 (2008) 2871e2885.

[33]Benajes J, Molina S, García A, Belarte E, Vanvolsem M. An investigation on RCCI combustion in a heavy duty diesel engine using in-cylinder blending of diesel and gasoline. Applied Thermal Engineering, vol. 63, 66-76, 2014.

[34]Desantes JM, Benajes J, García A, Monsalve-Serrano J. The Role of the In-Cylinder Gas Temperature and Oxygen Concentration over Low Load RCCI Combustion Efficiency. Energy, Volume 78, 15 December 2014, Pages 854-868.

[35]Dec J E, Yang Y. Boosted HCCI for high power without engine knock and with ultra-low NOx emissions using conventional gasoline. SAE Int. J. Engines, 2010, 3(1), 750–767.

[36]Cheng A, Upatnieks A, Mueller C. Investigation of Fuel Effects on Dilute, Mixing-Controlled Combustion in an Optical Direct-Injection Diesel Engine. Energy Fuels, 21 (4), pp 1989–2002, 2007.

Abbreviations

1-D: One-dimensional

ASTM: American Society of Testing and Materials

ATDC: After Top Dead Center

CAD: Crank Angle Degree

CA10: Cranck Angle at 10% mass fraction burned

CA50: Cranck Angle at 50% mass fraction burned

CA90: Cranck Angle at 90% mass fraction burned

CDC: Conventional Diesel Combustion

CO: Carbon Monoxide

COV_{IMEP}: Coefficient of Variation of the IMEP

CI: Compression Ignition

DI: Direct Injection

Diesel B7: Diesel fuel with 7% of biodiesel content by volume

DPF: Diesel Particulate Filter

EGR: Exhaust Gas Recirculation

EVC: Exhaust Valve Close

EVO: Exhaust Valve Open

EOI: End of Injection

E10-95: 95 ON gasoline with 10% of ethanol content by volume

E10-98: 98 ON gasoline with 10% of ethanol content by volume

E20-95: 95 ON gasoline with 20% of ethanol content by volume

E85: gasoline with 85% ethanol by volume

FSN: Filter Smoke Number

HC: Hydro Carbons

HCCI: Homogeneous Charge Compression Ignition

HD: Heavy Duty

HRF: High Reactivity Fuel

HTHR: High Temperature Heat Release

ICE: Internal Combustion Engine

IVC: Intake Valve Close

IVO: Intake Valve Open

LHV: Lower Heating Value

LNT: Lean NOx Trap

LRF: Low Reactivity Fuel

LTC: Low Temperature Combustion

MON: Motor Octane Number

ON: Octane Number

PM: Particulate Matter

PFI: Port Fuel Injection

PER: Premixed Energy Ratio

PPC: Partially Premixed Charge

PRR: Pressure Rise Rate

RCCI: Reactivity Controlled Compression Ignition

RON: Research Octane Number

RoHR: Rate of Heat Release

RI: Ringing Intensity

SCE: Single Cylinder Engine

SCR: Selective Catalytic Reduction

SoC: Start of Combustion

SoI: Start of Injection

SoI_{main}: Start of main Injection